AIAA JOURNAL
Vol. 35, No. 5, May 1997

Flap Side-Edge Noise: Acoustic Analysis of Sen's Model

Jay C. Hardin*
NASA Langley Research Center, Hampton, Virginia 23681
and
James E. Martin†
Christopher Newport University, Newport News, Virginia 23606

The two-dimensional flap side-edge flow model developed by Sen (Sen, R., "Local Dynamics and Acoustics in a Simple Model of Airfoil Lateral-Edge-Noise," AIAA Paper 96-1673, May 1996) is analyzed to reveal the noise-production potential of the proposed mechanism. The model assumes that a vortex will form at the equilibrium position off the side edge of the flap. The vortex is then perturbed away from the equilibrium position by incoming turbulence, causing it to oscillate and thus radiate sound. The noise field is calculated three-dimensionally by taking the flap to have a finite chord. Spectra and directivity of the far-field sound are presented. In addition, the effect of retarded time differences is evaluated. The parameters in the model are related to typical aircraft parameters and noise reduction possibilities are proposed.

Introduction

SOUND generated at the side edges of flaps is a very important, in some cases the most intense, source of airframe noise. The significance of this source began to be recognized in the late 1970s.[1] In particular, both Kendall and Ahyte[2] and Fink and Schlinker[3] showed that the flap side edges were more efficient noise radiators than the trailing edge source, which had been considered to dominate wing-produced noise up to that time. These early studies have recently been confirmed in an extensive series of tests.[4]

The appearance of this hitherto unsuspected source led to various attempts to understand and model the physics of the noise-generation process. Because one is particularly interested in flap side-edge noise on landing approach where the Mach number $M \cong 0.2$ is low, incompressible fluid-dynamic models can be employed to specify the acoustic sources. Hardin[5] suggested that the sound was produced by boundary-layer turbulence on the underside of the flap being swept around the edge by the tip flow and calculated the transient noise radiated by a single such event when the turbulent eddy was modeled by a point vortex and the flap by an infinitesimally thin half-plane. Howe[6] argued that the noise radiation was produced by an instability of the separation bubble formed on the upper surface of the flap and took into account the nearby presence of the undeflected portion of the flap. The "installation" or "proximity" effect was important to the radiation efficiency of the proposed flap-edge source. Howe's model was that of an infinitesimally thin half-plane with a small slot to represent the gap between the flap edge and the neighboring surface. Meecham[7] proposed that the thickness of the flap was important in moderating the accelerations and, hence, noise production by infinitesimally thin models and began modeling this effect by considering a vortex convecting around a right-angle corner.

Recently, Sen proposed a new physical mechanism for the flap-edge noise source[8] and a two-dimensional model to illustrate it. The model suggests that the flap-edge vortex itself can be excited into periodic oscillations as it is perturbed by a small secondary vortex or turbulent eddy. This model has several intriguing mathematical aspects and also appears to have physical plausibility based on flow visualization tests.[9] This paper is concerned with acoustic calculations based on Sen's model.

Sen's Flap-Edge Flow Model

Consider the geometry shown in Fig. 1a. The flap (viewed from the streamwise direction) is taken to be a slab of thickness $2s$ in the presence of which there exists a potential flow as well as a vortex Γ to represent the flap-edge vortex. The slab geometry has been studied by Clements,[10] who showed that the region exterior to the slab can be transformed into the upper half-plane shown in Fig. 1b via conformal mapping:

$$z = (2is/\pi)\left\{i\,\ell_n\left[i\lambda + (1-\lambda^2)^{\frac{1}{2}}\right] - \lambda(1-\lambda^2)^{\frac{1}{2}}\right\} \tag{1}$$

If the potential in the transform plane is taken as

$$w(\lambda) = \frac{-4sV_0}{\pi}\lambda\frac{-i\Gamma}{2\pi}\,\ell_n\left[\frac{\lambda-\lambda_0}{\lambda-\lambda_0^*}\right] \tag{2}$$

where $\lambda_0 = \zeta_0 + in_0$ is the position of the vortex and the asterisk indicates a complex conjugate, then the upwash velocity at the origin in the physical plane produced by the potential flow alone is V_0. It can then be shown that the vortex has an equilibrium point $(x_s, 0)$ in the physical plane where the upwash potential flow velocity is just balanced by the image vortex-induced velocity. This equilibrium point corresponds in the transform plane to the point $(0, n_s)$, where n_s is the real root of the cubic equation:

$$n_0^3 - 2\alpha n_0^2 + n_0 - \alpha = 0$$

where

$$\alpha = \frac{\Gamma}{16V_0 s} \tag{3}$$

is the nondimensional parameter that controls the dynamics of the flow. These equilibrium points are shown in Fig. 2 as a function of the parameter α.

A steady tip vortex flow would of necessity be found at these equilibrium points. However, the question arises as to what would happen if the tip vortex were perturbed away from the equilibrium point, say by lower surface vorticity being swept around the edge. This question is answered by the Kirchhoff–Routh path function,[11] which describes the path of the tip vortex. For this flow, the path function is

$$n_0 - \alpha\,\ell_n\left|n_0(1-\lambda_0^2)^{\frac{1}{2}}\right| = \text{const}$$

Contours of constant path function in the transform plane are shown in Fig. 3 (note the change in n scale on these plots) for different values of α. As can be seen, for smaller values of α, the

Presented as Paper 96-1674 at the AIAA/CEAS Aeroacoustics Conference, State College, PA, May 6–8, 1996; received June 1, 1996; revision received Jan. 15, 1997; accepted for publication Feb. 17, 1997.

*Senior Scientist, Fluid Mechanics and Acoustics Division, MS 462.
†Assistant Professor, Department of Mathematics, 50 Shoe Lane.

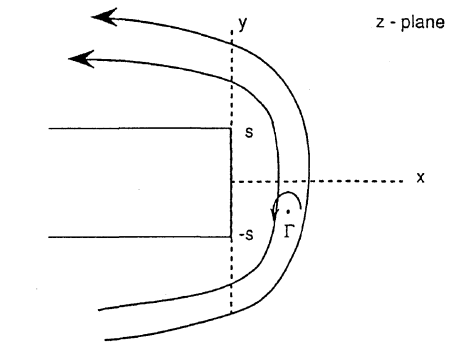

a) Physical plane

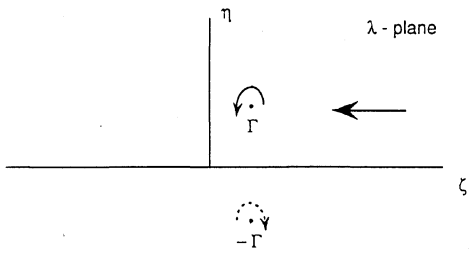

b) Transform plane

Fig. 1 Transformation geometries.

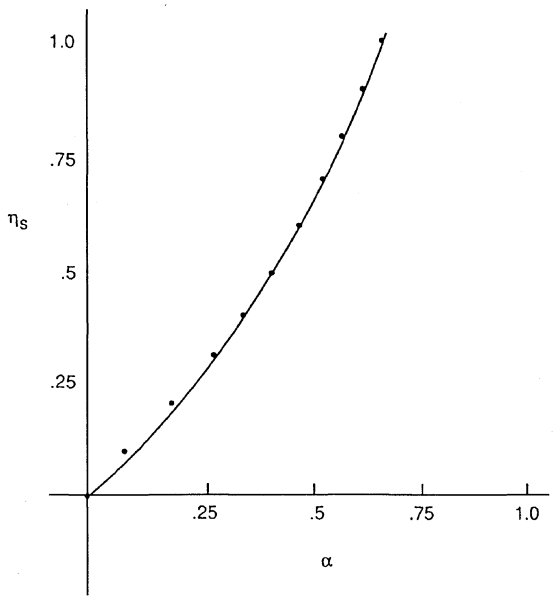

Fig. 2 Equilibrium points.

vortex paths form closed orbits about the equilibrium point, whereas for larger values of α, the paths diverge from the equilibrium point. In fact, the cutoff value is $\alpha = \frac{2}{3}$, with flows for which $\alpha < \frac{2}{3}$ exhibiting periodic oscillation of the tip vortex about its equilibrium point. These periodic orbits in the transform plane transform back to periodic orbits in the physical domain as shown in Fig. 4 for $\alpha = 0.3$. Here lengths have been nondimensionalized by the flap thickness $h = 2s$.

Of particular interest for noise generation is the period of these periodic orbits. In theory,[12] one should be able to determine the period analytically by writing a differential equation

$$\dot{r}^2 = f(r)$$

where r is the distance the vortex is displaced from its equilibrium point and integrating. However, whereas the required analysis is readily accomplished in the linearized case, the full nonlinear case is more problematic. Thus, the periods were determined numerically. Figure 5 is a plot of the nondimensional periods as a function of $r_0 = x - x_s$, which is the distance in the x direction that the vortex was initially displaced from its equilibrium position. Curves are shown for different values of the controlling parameter α given by Eq. (3). Note that these curves are reasonably independent of the initial displacement distance (i.e., size of the orbit) but do depend on α. In Fig. 5, time has been nondimensionalized by Γ/s^2. Thus, the Strouhal number of the periodic orbits, $Sr = fh/V_0$, becomes

$$Sr(\alpha) = 32\alpha/p(\alpha) \tag{4}$$

where $p(\alpha)$ is the nondimensional period shown in Fig. 5. Figure 6 is a plot of Eq. (4). Note that the Strouhal number is near one for $\alpha = 0.1$ but drops off to near one-tenth at $\alpha = 0.6$. Thus, the Strouhal number is strongly dependent on the characteristic parameter α.

This model does not take into account any vorticity that might be shed from the corners of the slab during the vortex motion. Recently, Howe[13] restudied the problem of a line vortex translating around the edge of a rigid half-plane and found that, if vorticity was continuously shed from the edge, to satisfy the Kutta condition there, the motion of the vortex was dramatically altered. In fact, the vortex no longer went around the edge, convecting away in partnership with the shed vorticity. One would not expect such dramatic changes in the flap-edge flow discussed here as it is known that the tip vortex does remain at the side edge of the flap. However, such considerations might somewhat alter the picture presented in this paper.

Acoustic Computations

For values of the controlling parameter α for which the tip vortex performs a periodic oscillation, periodic noise will be produced. The sound radiation can be calculated in several ways, given a knowledge of the vortex motion. Perhaps the simplest way is to use the Ffowcs Williams–Hawkings equation,[14] which, neglecting the quadrupole contribution as small compared to the dipole, becomes for this flow

$$\Box^2 p' = \frac{-\partial[pn_i\delta(f)]}{\partial x_i} + \frac{\partial}{\partial t}[\rho_0 v_n \delta(f)] \tag{5}$$

where p' is the acoustic pressure in the far field, $f = 0$ describes the flap surface, $\delta(f)$ is the Dirac delta function, n_i are the components of the unit normal vector $\bar{n}$ to the flap surface, p is the total pressure, ρ_0 is the density of the medium, and v_n is the normal velocity of the surface.

Consider the geometry shown in Fig. 7. The flap is taken to have finite chord c, and the origin of coordinates is at the center of the flap side face. The observer is at position $\bar{x}$, $\bar{y}$ is a variable that sweeps over the surface of the flap, and $\bar{r} = \bar{x} - \bar{y}$ is the source/observer vector. Using the free space Green's function, the wave equation, Eq. (5), can then be integrated by using the ideas of generalized function theory.[15] This solution is valid for the flight case of a body moving through an ambient medium past a stationary observer. However, it can be used to simulate the wind tunnel case where the observer is fixed with respect to the flap by assuming that, each time the solution is evaluated, the observer is moved to maintain the same position relative to the flap. In this case, the monopole (thickness noise) second term in Eq. (5) makes no contribution, and, for an observer in the acoustic far field, the solution may be written as

$$p'(\bar{x}, t) = \frac{1}{4\pi a_0}\int_{f=0}\left[\frac{\boldsymbol{n}\cdot\boldsymbol{r}}{r^2}\frac{\partial P}{\partial t}\right]_{\text{ret}} \mathrm{d}s \tag{6}$$

where $r = |\boldsymbol{r}|$, a_0 is the ambient speed of sound in the medium, the subscript ret indicates evaluation at the retarded time $t - r/a_0$, and, because the flow of interest is at low Mach number, the total pressure p has been approximated by the incompressible hydrodynamic pressure P. Thus, one needs to know only the incompressible pressure on the flap surface to calculate the resulting sound field. The surface pressure is not the source of the sound but merely contains the information about the true source, which is the motion of vorticity within the flow, necessary to calculate the resulting radiation field.

The hydrodynamic pressure everywhere in the field except where the vortex exists can be found from the Bernoulli theorem

$$\frac{\partial\phi}{\partial t} + \frac{q^2}{2} + \frac{P}{\rho_0} = \text{const}$$

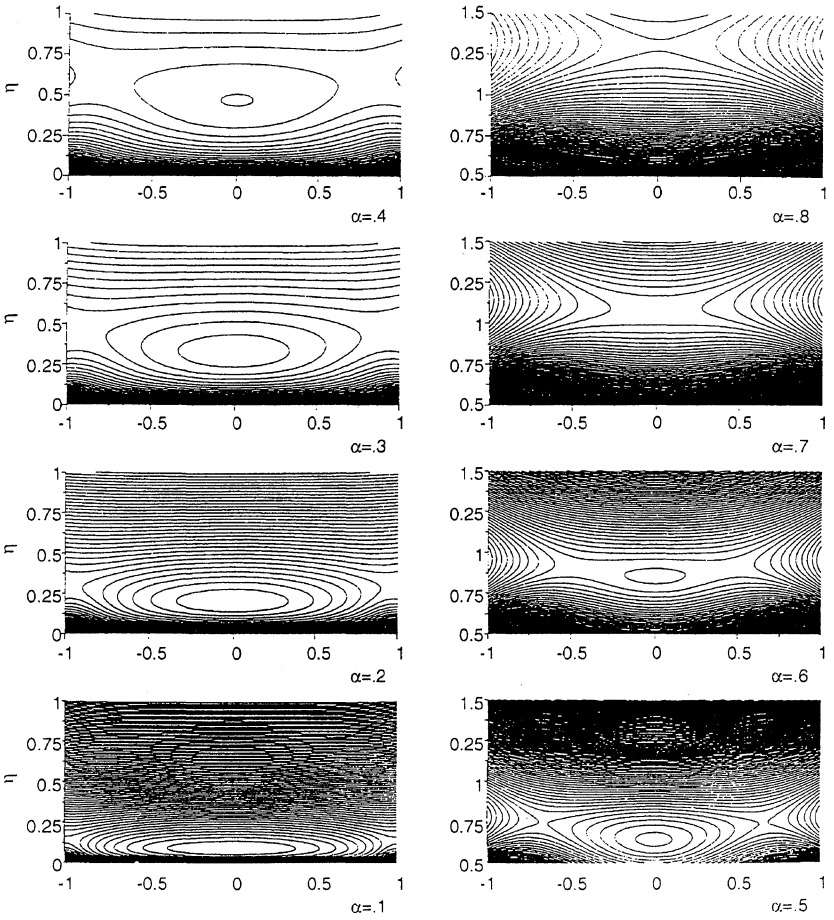

Fig. 3 Path function contours.

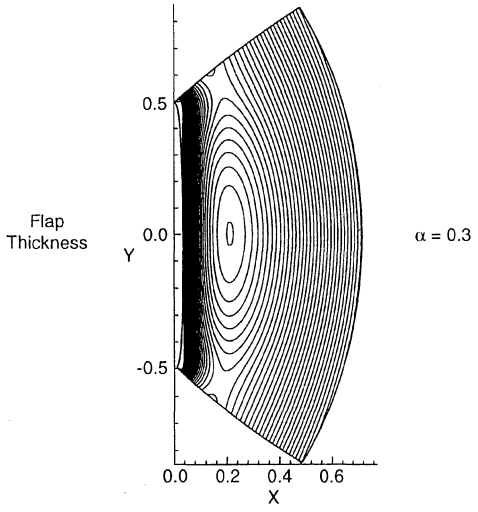

Fig. 4 Contours in the physical plane.

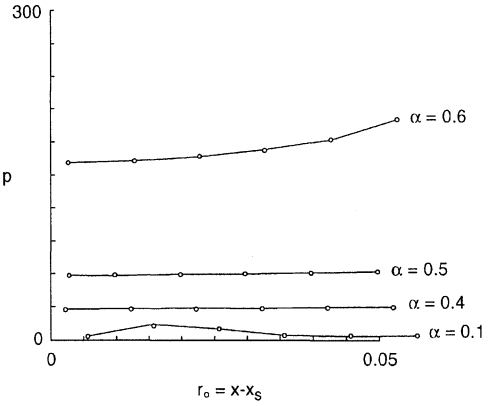

Fig. 5 Period of the orbits.

because both $\phi = \mathrm{Re}[w(\lambda)]$ and $q^2 = |(dw/d\lambda)(d\lambda/dz)|^2$ can be calculated from the conformal transformation, Eq. (1), and the complex potential, Eq. (2). On the surface of the flap, the hydrodynamic pressure is

$$P - P_0 = \frac{\rho_0 \Gamma}{\pi}\left[\frac{(\zeta - \zeta_0)\dot{\eta}_0 + \eta_0 \dot{\zeta}_0}{(\zeta - \zeta_0)^2 + \eta_0^2}\right] - \frac{\rho_0 V_0^2}{2|1 - \zeta^2|}\left[1 + \frac{4\alpha\eta_0}{(\zeta - \zeta_0)^2 + \eta_0^2}\right]^2 \tag{7}$$

where P_0 is the ambient pressure far from the edge of the flap. Note that Eq. (7) has the typical inviscid fluid characteristic of becoming unbounded at the corners (i.e., $\zeta = \pm 1$) of the flap. Although not unbounded, these low pressures are realistic based on recent steady-state computational results with the lowest pressure (lower than in the center of the vortex itself for the case calculated) occurring at the corner nearest the vortex. In the real world, these unbounded pressures predicted by the inviscid model of Eq. (7) are moderated by viscosity. Computationally, the infinities in the pressure are avoided by taking the grid points utilized in the numerical integration of Eq. (6) symmetrically placed close to, but not at, the corners of the flap. The sensitivity of the acoustic results to the placement of these points is evaluated below. Because the intent of this model is not to achieve a quantitative prediction of the magnitude of the noise generation, which is too much to expect from such a simple model, but merely to understand the mechanism, such an approximation should be sufficient.

Extensive acoustic calculations with Eq. (6) have been carried out for various values of the characteristic parameter α, vortex initial

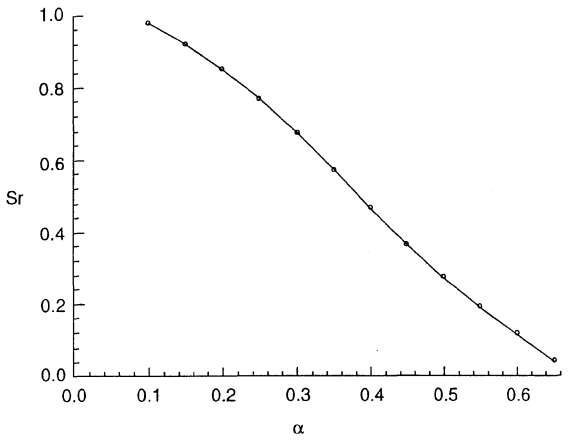

Fig. 6 Strouhal number of oscillations.

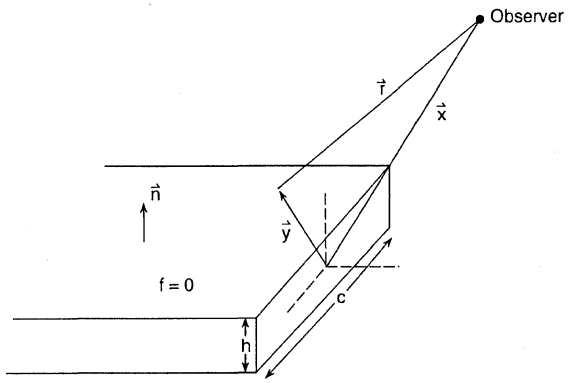

Fig. 7 Geometry for noise calculation.

positions, and observer locations. In carrying out the calculations, a finite chord length of 49.2 flap thicknesses was chosen for the flap and the assumption was made that the two-dimensional model flow would be found to describe the flow all along the length of the chord. Then, because the hydrodynamic pressure field given by Eq. (7) falls off rather slowly with distance (proportional to 1/distance) back along the span of the flap from the corners, $z = \pm is$, a convergence study was performed to determine how far the numerical integration should extend back along the span. Convergence was obtained on the order of 50 flap thicknesses. The panels used in the numerical integration were square with side 0.2. The top and bottom of the flap were tiled by 295 × 246 such panels and the flap edge contained 246 × 5 panels.

As an example of the acoustic results, Fig. 8 presents the normalized acoustic pressure time history as seen by an observer directly above the edge. The computation is initialized at a nondimensional time of $t = 0$, and no response is felt at the observer location until approximately $t = 15$, i.e., $a_0 h/\Gamma$ was set to unity. After that, a reasonably periodic acoustic signature of the periodic vortex motion develops. Note that this time history, which was observed at 15 flap thicknesses above the flap and calculated using the far-field approximate formula given by Eq. (6), appears to exhibit a bit of the characteristic nonlinear effects of steepening of the peaks and rounding of the troughs normally associated with propagation of high-amplitude acoustic waves. These effects would not be expected to appear in the present analysis as propagation effects are apparently embodied in the quadrupole term[16] of the Ffowcs Williams–Hawkings equation. Further, these effects do not seem to evolve but are present from the outset. Apparently their presence here is due to numerical integration of the singularity at the flap corners, as the pressure field is not symmetric about the corner. Although such corners can be handled rigorously,[15] it was not done here as the problem would not exist in a more realistic model. To evaluate the sensitivity of the results to the numerical integration near the corners, the width of the panels in the spanwise direction was changed. Figure 9 is a plot of the maximum excursion (i.e., $p'_{\max} - p'_{\min}$) of the calculated acoustic

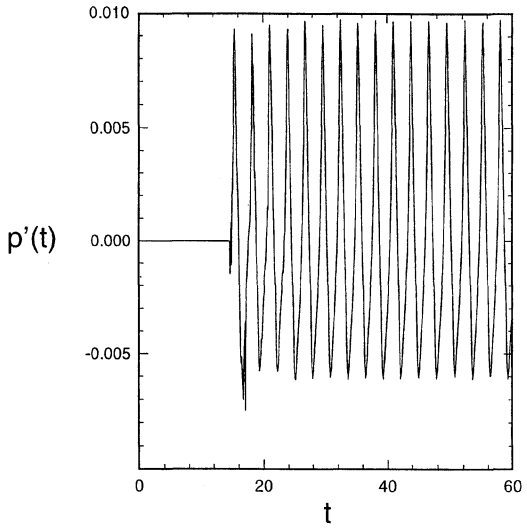

Fig. 8 Acoustic pressure time history: $\alpha = 0.1$, $x_{obs} = 0.0$, and $y_{obs} = 15.0$.

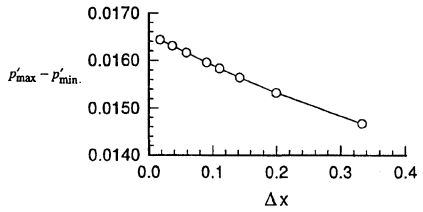

Fig. 9 Maximum acoustic pressure excursion as a function of panel width.

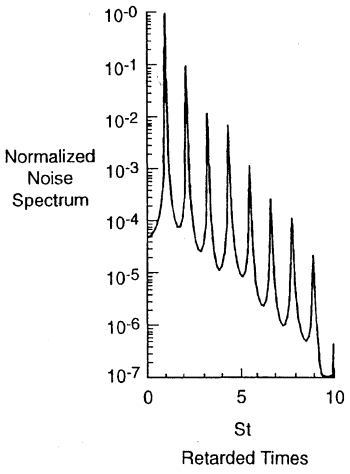

Fig. 10 Normalized acoustic spectrum.

pressure as a function of panel width for $\alpha = 0.1$. As shown, the maximum excursion increases as the panel width is decreased from its nominal value of 0.2, but no dramatic changes occur even for a factor of 10 reduction.

The normalized spectrum of the time history of Fig. 8 is shown in Fig. 10. This spectrum was calculated from 512 points covering precisely seven periods of the periodic signal. Note the typical periodic spectrum containing the fundamental frequency and its harmonics, with the highest harmonic 10 dB down on the fundamental amplitude. A study was also made of the effect of neglecting retarded time differences in the analysis, as this is an assumption that is often made to simplify the calculations. Figure 11 is the spectrum produced for the same case as that shown in Fig. 10 but with retarded time differences over the surface of the flap neglected. Thus, the spectra of Figs. 10 and 11 are directly comparable. Note that the levels of the harmonics are significantly changed by this approximation. Thus, accurate calculation of the spectral components, even at low Mach numbers where the wavelengths tend to be long, requires proper accounting for retarded time differences.

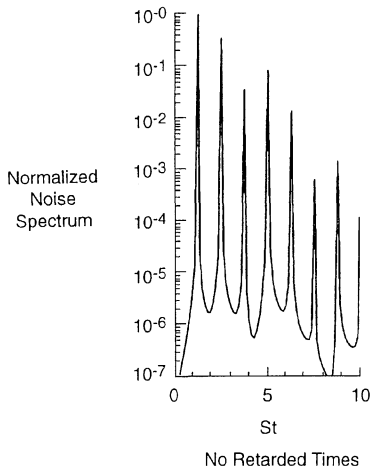

Fig. 11 Noise spectrum with retarded time differences neglected.

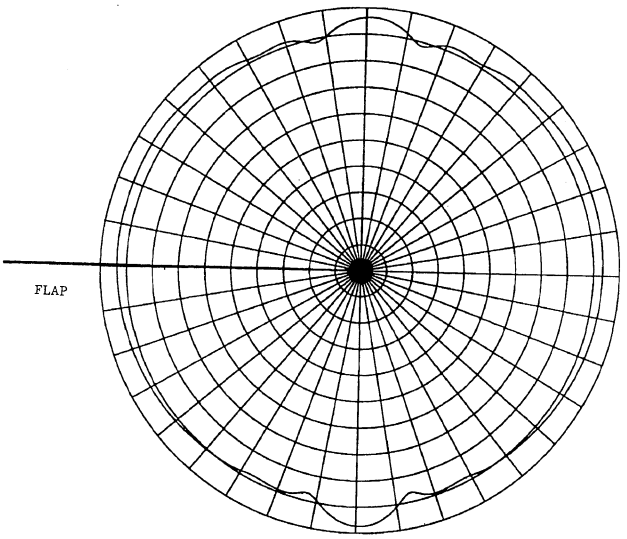

Fig. 12 Directivity in spanwise plane.

Finally, the directivity pattern of the noise radiation is of interest. This pattern was calculated on a circular arc of nondimensional radius $|\bar{x}| = 2000$ to be well outside the equivalent source distribution region. Figure 12 displays the directivity pattern in a spanwise plane perpendicular to the flap edge. The directivity is nearly circular with only slight peaks normal to the flap. Apparently the valley in the "baffled dipole" directivity pattern of trailing edge noise[1] is filled in by dipoles on the flap-side edge. It should be recalled, however, that only the hydrodynamic pressure fluctuation was utilized in the integration. Because these fluctuations fall off rapidly with distance from the edge, much of the flap surface will experience only acoustic pressure fluctuations. Just such a case where part of the surface appearing in the integral of Eq. (6) is far from the region of hydrodynamic pressure fluctuations was discussed by Powell,[17] who observed that the acoustic pressure fluctuations should then be taken into account in the integral.

Implications of Model for Flap-Edge Noise Generation

Although Sen's model[8] is a highly simplified two-dimensional model of a very complex three-dimensional flap flowfield, it is of interest to relate the model as closely as possible to the real aircraft geometry and to consider its implications for the flap-edge noise generation phenomenon. Recall first that the behavior of the model was governed by the characteristic parameter

$$\alpha = \frac{\Gamma}{16V_0 s} = \frac{\Gamma}{8V_0 h}$$

where Γ is the vortex strength, V_0 is the upwash velocity at the flap edge, and h is the flap thickness. Periodic orbits exist for $\alpha < \frac{2}{3}$. For these orbits, the Strouhal number is reduced as α is increased, as shown in Fig. 6. Analysis of Eq. (7) also indicates that the nondimensional source strength $\partial P/\partial t$ is proportional to $\alpha\Gamma\rho_0 V_0^2/h^2$ to lowest order in α. Thus, the integrated acoustic intensity I is proportional to $(\Gamma\rho_0 V_0^2/a_0 r)^2(\alpha^2 c^2/h^2)$, indicating the expected dipole velocity dependence.

To relate this model to a typical aircraft geometry, recall that the flaps are normally deployed at some angle-of-attack δ to the freestream. Although the inflow to the flap will be highly dependent upon the upstream geometry, at the high angles of deflection of interest, one might approximate the upwash velocity V_0 as $U_0 \sin\delta$, where U_0 is the incoming flow velocity (or flight speed of the aircraft). The vortex strength Γ is determined by the lift distribution on the flap and can be related to the jump in the sectional lift coefficient at the flap edge. However, as a first approximation, one might take $\Gamma = L/\rho_0 U_0$, where $L = C_L(\delta)\rho_0 U_0^2 c/2$ is the lift force per unit span on the flap and $C_L(\delta)$ is the lift coefficient for the flap. Thus, in typical aircraft parameters,

$$\alpha = \frac{C_L(\delta)c}{16h\sin\delta} \tag{8}$$

Note that this relation displays no explicit dependence upon incoming flow velocity U_0. Now, even when the flap is undeflected, it will be carrying lift. Thus, α will be very large for small deflection angles, implying that no equilibrium point exists and that periodic sound will not be generated by this mechanism. Presumably, in this case, vorticity produced at the tip of the flap will be swept away, as suggested by Fig. 3, and no concentrated tip vortex will form. This analysis thus predicts that there may be a critical flap deflection angle below which the proposed mechanism will not be present. However, as the flap is further deflected, α will decrease. Insertion of typical values [$\delta = 30$ deg, $C_L(\delta) = 0.3$ for the flap, $h/c = 0.12$] into Eq. (8) suggests an α value of approximately 0.34, well within the range where an equilibrium point must exist.

Because at typical landing approach speeds and flap deflection angles, $\alpha < \frac{2}{3}$, the present mechanism can generate periodic sound at the flap edge. The typical aerodynamic Strouhal number

$$Sr = fh/U_0 \cong Sr(\alpha)\sin\delta$$

governs the frequency of the sound produced, where $Sr(\alpha)$ is shown in Fig. 6. At $\alpha = 0.34$ and $\delta = 30$ deg, this analysis yields $Sr = 0.3$. Although clear data on flap side-edge noise generation are difficult to obtain, measured surface pressure spectra (see Ref. 18) on a blunt-tipped airfoil displayed peaks at $0.8 < Sr < 1.3$, which implies a very small value of α. The behavior of these data as a function of δ is ambiguous.

Unless some frequencies are preferable to others for certification considerations, one would then want to make the intensity

$$I \sim (\alpha^2 c^2/h^2)\sin^4\delta \sim C_L^2(\delta)(c^4/h^4)\sin^2\delta$$

as small as possible. Clearly, the obvious way to accomplish such noise reduction is to reduce the chord or increase the thickness of the flap. A 10% reduction in the chord or a 10% increase in the thickness would reduce the sound intensity by 1.66 dB, and doing both would result in a 3.49-dB noise reduction. However, there the aerodynamic/acoustic tradeoffs are apparent as all of the variables are coupled by the lift necessary to be produced by the flap. In particular, the variation of $C_L(\delta)$ and $C_D(\delta)$ with variations in c and h is of paramount importance.

Conclusions

The simple two-dimensional flap-edge flow model suggested by Sen has been evaluated to reveal its noise production characteristics. The Ffowcs Williams–Hawkings equation was integrated over the surface of the flap by using surface pressures produced by the model. The noise generation was found to depend on a characteristic parameter, α, which could be related to typical aircraft parameters. Periodic dipole sound containing the fundamental frequency and several nonnegligible harmonics is produced at a given value of α. The intensity of this sound can be reduced by reducing the chord or increasing the thickness of the flap. However, these parameters are constrained by the necessary lift generation of the flap.

Acknowledgment

This research was supported in part by NASA under Contract NAS1-19480 while the second author was in residence at the Institute for Computer Applications in Science and Engineering, NASA Langley Research Center.

References

[1]Crighton, D. G., "Airframe Noise, Aero-acoustics of Flight Vehicles: Theory and Practice, Volume 1: Noise Sources," NASA RP 1258, Aug. 1991, pp. 391–447.

[2]Kendall, J. M., and Ahtye, W. F., "Noise Generation by a Lifting Wing/Flap Combination at Reynolds Numbers to 2.8×10^6," AIAA Paper 80-0035, Jan. 1980.

[3]Fink, M. R., and Schlinker, R. H., "Airframe Noise Component Interaction Studies," AIAA Paper 79-0668, March 1979.

[4]Sen, R., "Assessment of the NASA ANOPP Method of Airframe Noise Prediction from a Noise Reduction Standpoint," The Boeing Co., Boeing Rept. D681619TN, Seattle, WA, Oct. 1995.

[5]Hardin, J. C., "Noise Radiation from the Side-Edges of Flaps," *AIAA Journal*, Vol. 18, No. 5, 1980, pp. 549–552.

[6]Howe, M. S., "On the Generation of Side-Edge Flap Noise," *Journal of Sound and Vibration*, Vol. 80, No. 4, 1982, pp. 553–573.

[7]Meecham, W. C., "Aerosound from Corner Flow and Flap Flow," *AIAA Journal*, Vol. 21, No. 2, 1983, pp. 228–234.

[8]Sen, R., "Local Dynamics and Acoustics in a Simple Model of Airfoil Lateral-Edge-Noise," AIAA Paper 96-1673, May 1996.

[9]Storms, B. L., Takahasi, T. T., and Ross, J. C., "Aerodynamic Influence of a Finite-Span Flap on a Simple Wing," Society of Automotive Engineers, SAE Aerotech '95, Paper 95-1977, Los Angeles, CA, Sept. 1995.

[10]Clements, R. R., "An Inviscid Model of Two-Dimensional Vortex Shedding," *Journal of Fluid Mechanics*, Vol. 57, Pt. 2, 1973, pp. 321–336.

[11]Saffman, P. G., *Vortex Dynamics*, Cambridge Univ. Press, Cambridge, England, UK, 1992, pp. 123–130.

[12]Synge, J. L., and Griffith, G. A., *Principles of Mechanics*, 3rd ed., McGraw–Hill, New York, 1959, p. 328.

[13]Howe, M. S., "Emendation of the Brown and Michael Equation, with Application to Sound Generation by Vortex Motion near a Half Plane," *Journal of Fluid Mechanics*, Vol. 329, 1996, pp. 89–102.

[14]Ffowcs Williams, J. E., and Hawkings, D. L., "Sound Generation by Turbulence and Surfaces in Arbitrary Motion," *Philosophical Transaction of the Royal Society of London, Series A: Mathematical and Physical Sciences*, Vol. 264, No. 1151, 1969, pp. 321–342.

[15]Farassat, F., "Introduction to Generalized Functions with Applications in Aerodynamics and Aeroacoustics," NASA TP 3428, May 1994.

[16]Brentner, K. S., and Holland, P. C., "An Efficient and Robust Method for Computing Quadrupole Noise," *Proceedings of the American Helicopter Society 2nd International Aeromechanics Specialist Conference* (Fairfield County, CT), American Helicopter Society, 1995.

[17]Powell, A., "Aerodynamic Noise and the Plane Boundary," *Journal of the Acoustical Society of America*, Vol. 32, No. 8, 1960, pp. 982–990.

[18]McInerny, S. A., and Meecham, W. C., "Pressure Fluctuations in the Tip Region of a Blunt-Tipped Airfoil," *AIAA Journal*, Vol. 28, No. 1, 1990, pp. 6–13.

S. Glegg
Associate Editor